Exploring the Maximum Allowable Oxidation and Peak Cladding Temperature Limits of Cr Coated Accident Tolerant Fuel Cladding

SungHoon Joung[a], Youho Lee[a*]
[a] *Department of Nuclear Engineering, Seoul National University, Gwanak-ro 1, Gwanak-gu, Seoul 08826, Republic of Korea*

[*] *Corresponding author: leeyouho@snu.ac.kr*

***Keywords :** Accident tolerant fuel (ATF), Cr-coated cladding, Post quench ductility, ECCS criteria, Failure mode

1. Introduction

The current Emergency Core Cooling System (ECCS) criteria have been established by the U.S Nuclear Regulatory Commission (U.S.NRC). These criteria limit the Equivalent Cladding Reacted (ECR) and Peak Cladding Temperature (PCT) to 17% and 1,204°C respectively, to ensure the nuclear fuel safety. Following the Fukushima accident, Accident Tolerant Fuel (ATF) cladding has emerged to prevent cladding from steam oxidation. Cr-coated Zircaloy cladding is considered a most promising option currently under development for near-term commercialization. However, applying the same criteria, such as PCT and ECR, to Cr-coated ATF introduces critical uncertainties due to existing knowledge gaps. This study addresses these gaps by conducting a comprehensive assessment of Post Quench Ductility (PQD), considering various types of zircaloy, including Cr-coated ATF. Furthermore, the study examines how the Zr-Cr eutectic melting affects the ductility of Cr-coated ATF, in order to determine the applicable PCT limit for Cr-coated ATF.

2. Methods and Results

2.1 Materials

The PQD experiment was carried out with various types of zircaloys, including Zircaloy-4, Opt. ZIRLO™, and HANA-6 alloy. To evaluate the residual ductility of the Cr-coated ATF after oxidation and quenching, Cr-coated Zircaloy-4, Cr and Cr/CrN bi-layer coated Opt. ZIRLO™, and Cr-coated HANA-6 were prepared. The composition of each alloy and dimensions were listed in **Table I**. The specimens were prepared to a length of 8mm for the PQD experiment. The coating on all types of specimens has a dense appearance without any voids, and they have a fairly uniform thickness.

Table I: Chemical composition and dimensions of the various claddings examined in this study.

Alloy	Coating method	Nb [wt%]	Sn [wt%]	Fe [wt%]	OD [wt%]	δ [wt%]	δ_{Cr} [μm]
Zircaloy -4	Bare	-	1.3-1.5	0.2	10.75	0.75	-
	Cr (magnetron)						9.2± 0.2
Opt. ZIRLO ™	Bare	1.0	0.7	0.1	9.15	0.57	-
	Cr (magnetron)						18.8 ±0.7
	Cr/CrN (magnetron)						20.1 ±0.4 /7.3 ±0.1
HANA-6	Bare	1.1	-	-	9.5	0.57	-
	Cr (AIP)						8.9± 0.6
	Cr (AIP)						19.0 ±0.3

2.2 Experimental setup
2.2.1 Steam oxidation experiments

The specimens were cleaned with ethanol and de-ionized water before oxidation. The weight of each specimen was measured using a balance both before and after oxidation. Following the weight measurement, the specimens were oxidized in high temperature steam oxidation environment using experiment facility which is designed to simulate loss of coolant accident (LOCA), as shown in **Fig. 1(a).** The experiment facility has been validated by a number of previous studies .

The specimens were placed in a holder and introduced into a pre-heat furnace. They were then oxidized at 1204±5°C for a specific time according to the experimental conditions. A K-type thermocouple was attached to a dummy specimen to measure the temperature of specimens during steam oxidation process. The temperature history of the specimens is shown in the **Fig. 1(b)**. The mass flux of steam entering into the furnace was 3.94 [mg/cm^{2}s]. This flow rate was is within the recommended range provided by the U.S. NRC. The oxidized specimens were cooled down to 800°C at a rate of 2°C/s to 4°C/s, by introducing an additional steam and argon. When the temperature of specimens reached to 800°C, the specimens were quenched in boiling water to mimic the reflood

quenching of the claddings upon the activation of ECCS rejection.

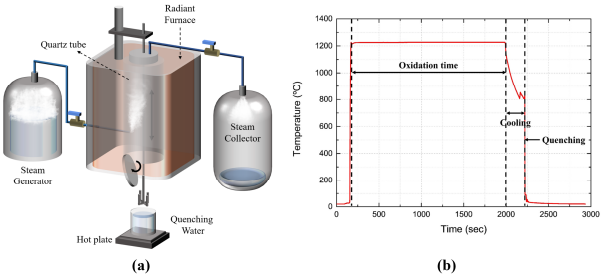

Fig. 1. LOCA experimental setup and temperature profile, (a) Schematic of LOCA simulated facility (b) Temperature profile during LOCA simulated experiment

2.2.2 Ring compression test (RCT)

After the high temperature steam oxidation, Ring Compression Test (RCT) was conducted to evaluate the residual ductility. A schematic diagram of RCT facility is shown in the **Fig. 2(a)**. The temperature of the top, bottom, left and right sides of the specimen were maintained within 135±3°C. The specimens were compressed at a displacement rate of 0.033 mm/s compliance with U.S.NRC's experimental protocol .

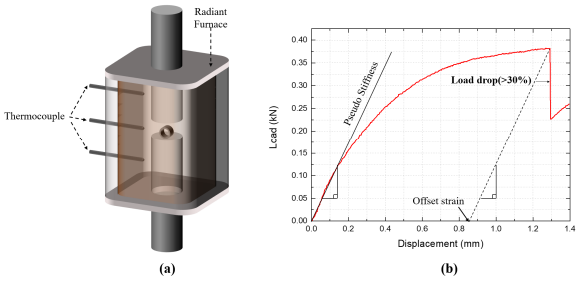

Fig. 2. Ring compression test facility and load-displacement curve, (a) Schematic of RCT facility (b) A load-displacement curve and parameters.

2.3 Applicable ECR limit for Cr-coated ATF

Figure 3 presents the offset strains of uncoated HANA-6 and Cr-coated HANA-6 specimens based on measured WG-ECR. Results of other types of claddings are included in the Appendix **(Fig. A)**. The ductility of the specimens decreases as the measured WG-ECR increases. The limit of measured WG-ECR for each specimen is determined by finding an intersection point between the ductile to brittle transition line proposed by U. S. NRC, which is shown as black solid line in **Fig. 3**, and the fitted curve of experimental data (dashed line).

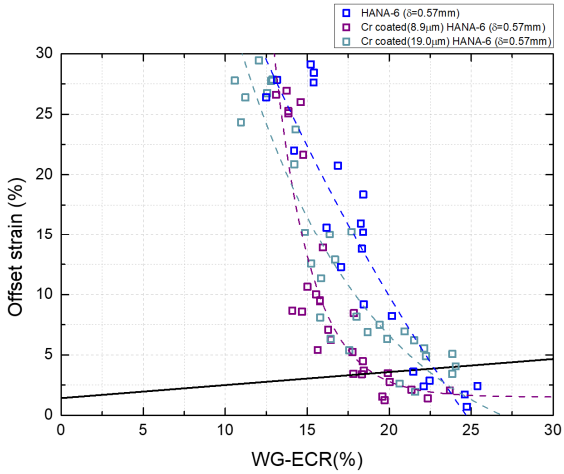

Fig. 3. measured WG-ECR to offset strain curve for bare HANA-6 and Cr coated HANA-6 with ductile to brittle criteria from U.S. NRC.

Table II provides a summary of the ductile to brittle transition WG- ECR limits obtained in this study. The results indicate that the measured WG-ECR limits of coated specimens (Cr and Cr/CrN) consistently decrease compared to their bare cladding. On average, there is a reduction of 3% (ΔECR). Yet, the results should not be misinterpreted: the time needed to reach the measured WG-ECR limit is still increased for coated claddings due to single-side oxidation. Also, As can be shown in HANA-6 data (**Fig. 3 and Table II**), The measured WG-ECR limit for Cr-coated HANA-6 with a thinner coating (8.9 μm) is decreased compared to the Cr-coated HANA-6 with a thicker coating (19.0 μm). This demonstrates a sensitivity to coating thickness for residual ductility of Cr-coated ATF.

Table II: Ductile to brittle transition measured WG-ECR limits

Alloy	Coating method	δ_{Cr} [μm]	measured WG-ECR limit [%]
Zircaloy-4	Bare	-	20
	Cr (magnetron)	9.2±0.2	15
Opt. ZIRLO™	Bare	-	24
	Cr (magnetron)	18.8±0.7	20
	Cr/CrN (magnetron)	20.1±0.4/7.3±0.1	19
HANA-6	Bare	-	23
	Cr (AIP)	8.9±0.6	19
	Cr (AIP)	19.0±0.3	22

Characteristics of crack propagation under RCT was investigated using Digital Image Correlation (DIC). Figure 4 show the major (through-wall) crack responsible for major load drop. For all tested claddings, cracks initiated at either 6 o'clock or 12 o'clock position regardless of coating and types of claddings.

For uncoated claddings, these initial cracks developed into major cracks which were responsible for the major load drop in RCT. The maximum tensile stresses

applied to these positions during RCT for cylindrical specimens, which retain a fairly cylindrical shape even under deformation **(Fig. B in Appendix)**. As a result, for uncoated claddings, the maximum tensile stress is applied to the most brittle phase (ZrO_2), leading to crack propagation at the 6 o'clock or 12 o'clock positions. However, A different major crack behavior was observed for the coated claddings. Same with the uncoated cladding, cracks initiate at the inner surface of either 6 or 12 o'clock positions. However, the major crack develops at either 3 o'clock or 9 o'clock positions as shown in **Fig. 4(b)**. This behavior was consistently observed regardless of types claddings tested in this study. Cracks developing from the 3 or 9 o'clock positions contribute to the observed decrease in the ECR limit of Cr-coated claddings.

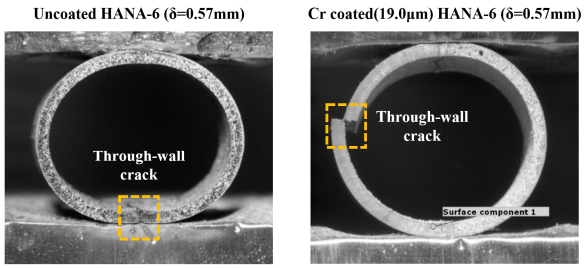

Fig. 4. Major crack behavior during RCT. (a) uncoated HANA-6 with 20% measured WG-ECR, (b) Cr-coated (19.0 μm) HANA-6 with 20% measured WG-ECR.

Figure 5 shows the crack morphologies for Cr-coated HANA-6 with 20% measured WG-ECR. As can be seen, the cracks developed at 3′o clock or 9′o clock, initiating from the thin $ZrCr_2$ layer formed during the oxidation of Cr-coated specimens. Therefore, the thin cracks initiated in the $ZrCr_2$ are responsible for the early major propagation compate to bare claddings. Furthermore, **Figure 5** shows the coating thickness effect for residual ductility of post-LOCA coated specimens. As shown in **Fig. 3 and Table II**, The measured WG-ECR limit for Cr-coated HANA-6 with a thinner coating (8.9 μm) is decreased compared to the Cr-coated HANA-6 with a thicker coating (19.0 μm). It means the earlier major crack occurred in the Cr-coated claddings with thinner Cr coating. Coating thickness changes the flux of oxygen diffusion, thereby affects the oxygen concentration in the Zr martix near the $ZrCr_2$ layer. **Fig. 5(c)** shows oxygen concentration of Zr matrix near $ZrCr_2$ layer with 20 % measured WG-ECR. The oxygen concentration in Zr matrix for the thinner Cr coating (8.9 μm) is higher than that of the thicker one. This occurs because as the Cr coating thickness increases, the distance that oxygen have to reach the Zr matrix becomes greater, leading to a reduced oxygen concentration within the Zr matrix.

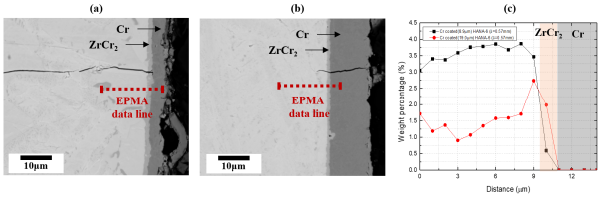

Fig. 5. Crack morphologies and oxygen concentration of Zr matrix near the interface between Zr and Cr coating for Cr-coated HANA-6 with 20% measured WG-ECR. (a) Cr coated (8.9μm) HANA-6, (b) Cr-coated (19.0 μm) HANA-6, and (c) oxygen concentration.

Figure 6 summarizes ECR limits obtained in this study and current ECR limits of bare Zircaloy by U.S. NRC. Cr coated (8.9μm) HANA-6 can serve as the lowest envelope (ECR 19 %) of ECR limits for tested coated Zircaloys. Therefore, the current ECR limit of 17% can conservatively applicable for the ECR limit of modern base Zircaloy materials (Opt. ZIRLO™ and HANA-6). Furthermore, it shows that the ECR limit of Cr-coated ATF remains constant as long as the integrity of the coating is intact, as it does not pick up hydrogen during steady-state conditions.

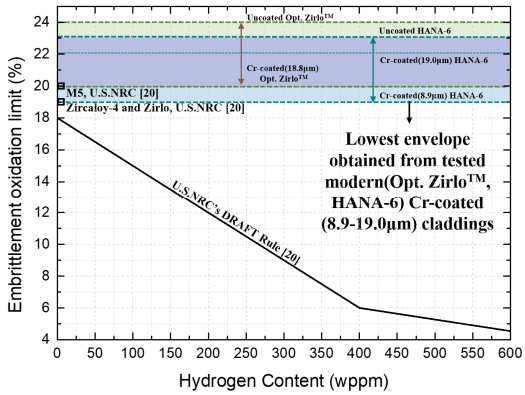

Fig. 6. Comparison of the current ECR limit and obtained ECR limit in this study.

2.4 Applicable PCT limit for Cr-coated ATF

The Peak Cladding Temperature (PCT) of conventional zircaloy is limited to 1,204°C, considering various phenomena such as the ductility of the cladding, runaway oxidation, and the melting of zircaloy. Most phenomena do not significantly differ in setting the PCT for Cr-coated ATF, which has Zircaloy as its matrix. However, the Zr-Cr eutectic melting has emerged as a new safety concern related to Cr-coated ATF. If this phenomenon is same as typical melting, then the PCT of Cr-coated ATF should be completely revised. However,

this phenomenon was revealed as a embrittlement [8]. Therefore, this study assesses the effect of Zr-Cr eutectic melting on the PCT for Cr-coated ATF, utilizing both bare HANA-6 and Cr-coated HANA-6 specimens. The same experimental facility (**Fig. 1**) was utilized to expose the Cr-coated specimens to temperatures above the onset temperature of eutectic melting. **Figure 7** shows the temperature history of the specimens.

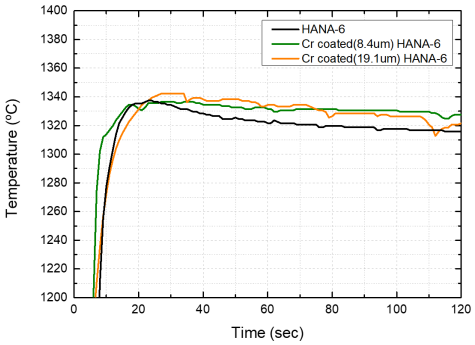

Fig. 7. Temperature profile during oxidation to examine the impact of Zr-Cr eutectic melting on the ductility of Cr-coated ATF.

Figure. 8(a) shows the offset strain-time curve of post-eutectic Cr-coated HANA-6 and post-oxidized HANA-6. The residual ductility of all types of claddings are quite decreased (**Fig. 8(b)**). However, the difference between bare and Cr-coated HANA-6 is negligible. Therefore, this indicates that the effect of the eutectic melting on the residual ductility of the coated claddings is limited.

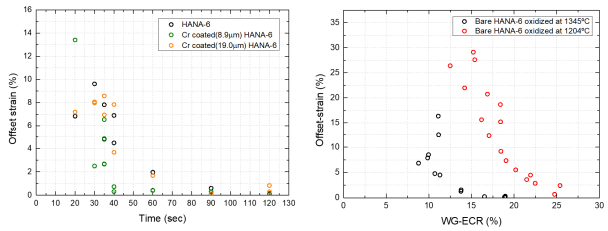

(a) (b)

Fig. 8. (a) Offset strain - time curve for bare HANA-6, Cr coated(8.9μm) HANA-6, and Cr coated(19.0μm) HANA-6. (b) Ductility assessment result of bare HANA-6 oxidized at different temperature (1,204℃ and 1,345℃).

EPMA analysis was conducted to investigate the oxidation temperature effect on the ductility. The thickness of each layer (α+β and prior β-layer) and the average oxygen concentration in each layer were analyzed across various ECR ranges (**Fig. 10**). **Figure. 9** shows the cross sectional image and the oxygen concentration within this layer. In **Fig. 9,** we can find that the thickness of ductile layer oxidized at 1,345°C is thicker. However, its oxygen concentration is increased. It can be attributed to the rate of oxygen diffusion, which is influenced by the oxidation temperature. It indicates that the oxygen concentration of the prior-β layer has increased. This indicates that the quality of the prior-β layer decreases as oxidation occurs at higher temperatures.

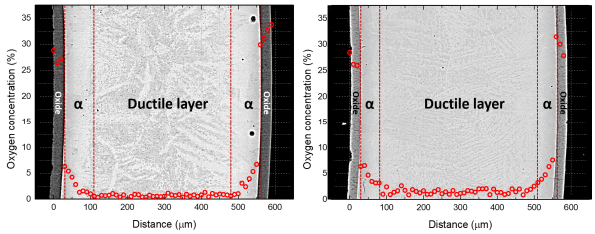

(a) (b)

Fig. 9. Cross sectional image and oxygen concentration of (a) HANA-6 oxidized at 1,204℃ with 11% ECR and (b) HANA-6 oxidized at 1,345℃ with 11% ECR.

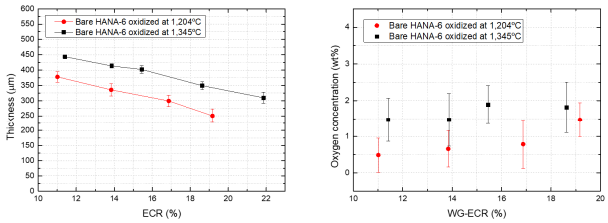

(a) (b)

Fig. 10. Comparison of (a) thickness of ductile layer and (b) average oxygen concentration in the ductile layer (prior-β layer) of oxidized specimens oxidized at different temperature (1,204℃ and 1,345℃)

3. Conclusions

This study investigated the applicable ECR and PCT limits for Cr-coated ATF. Experiments to find ECR limit followed the U.S. NRC's PQD test protocols for Emergency Core Cooling System (ECCS) criteria, aiming to determine the appropriate limit for Cr-coated ATF. Additionally, experiments were conducted to assess the applicable PCT limits with a primary focus on the impact of Zr-Cr eutectic melting, a new safety concern in Cr-coated ATF, on ductility of cladding. The conclusions are as follows:

- The ECR limits of coated specimens was lower than those of the base cladding materials due to early load drop during RCT. Cracks initiating from $ZrCr_2$ layer at 3 or 9 o'clock positions primarily contribute to this load drop, leading to reduced ECR limits for tested coated ATF. These crack propagation was promoted by increased oxygen concentration in the Zr matrix.
- The maximum attainable ECR limit for coated ATF is influenced by its base cladding materials. While 19% ECR (the limit for Cr-coated (8.9μm) HANA-6) could

serve as a conservative ECR limit, it exceeds the current ECR criteria of 17%. Also, considering the limited impact of marginal increases in ECR limit on nuclear safety. regulation. Adopting current 17% of ECR limit for Cr-coated ATF should be simple and effective.

- The impact of Zr-Cr eutectic melting on the residual ductility of the Cr-coated ATF is limited, as oxidation-induced embrittlement predominates at the onset temperature of Zr-Cr eutectic melting. Faster oxygen diffusion during oxidation at the onset temperature of eutectic melting makes the thicker ductile layer compared to oxidized specimen at the 1,204℃. However, this also results in an increase in oxygen concentration within the ductile layer, leading to a decrease in its quality.
- This research revealed that the impact of the Zr-Cr eutectic melting on the residual ductility of Cr-coated ATF is limited. However, it is important to consider various degradation phenomena, including runaway oxidation due to ZrO_2 phase transformation near the conventional 1204°C PCT. Therefore, applying the conventional 1204°C PCT to Cr-coated ATF remains a rational and effective.

REFERENCES

[1] D. Hobson, "Ductile-brittle behavior of Zircaloy fuel cladding," OAK RIDGE NATIONAL LAB., TENN., 1972.

[2] D. Hobson and P. Rittenhouse, "EMBRITTLEMENT OF ZIRCALOY-CLAD FUEL RODS BY STEAM DURING LOCA TRANSIENTS," Oak Ridge National Lab., Tenn., 1972.

[3] H. Yook and Y. Lee, "Post-LOCA ductility assessment of Zr-Nb Alloy from 1100 degrees C to 1300 degrees C to explore variable peak cladding temperature and equivalent cladding reacted safety criteria," (in English), *J Nucl Mater,* vol. 567, Aug 15 2022.

[4] H. Yook, K. Shirvan, B. Phillips, and Y. Lee, "Post-LOCA ductility of Cr-coated cladding and its embrittlement limit," (in English), *J Nucl Mater,* vol. 558, Jan 2022.

[5] S. Joung, J. Kim, M. Ševeček, J. Stuckert, and Y. Lee, "Post-quench ductility limits of coated ATF with various zirconium-based alloys and coating designs," *J Nucl Mater,* vol. 591, p. 154915, 2024.

[6] USNRC. Regulatory Guide 1.223-Determing post quench ductility," Washington. D.C., USA, 2018.

[7] NUREG/CP-6967-Cladding Embrittlement During Postulated Loss-of-Coolant Accidents " U.S.NRC, 2008.

[8] B. Kweon and Y. Lee, "Experimental Investigation of Eutectic Formation in Cr coated Accident Tolerant Fuel Cladding and its Safety Implications", KNS, May, 2024.

APPENDIX

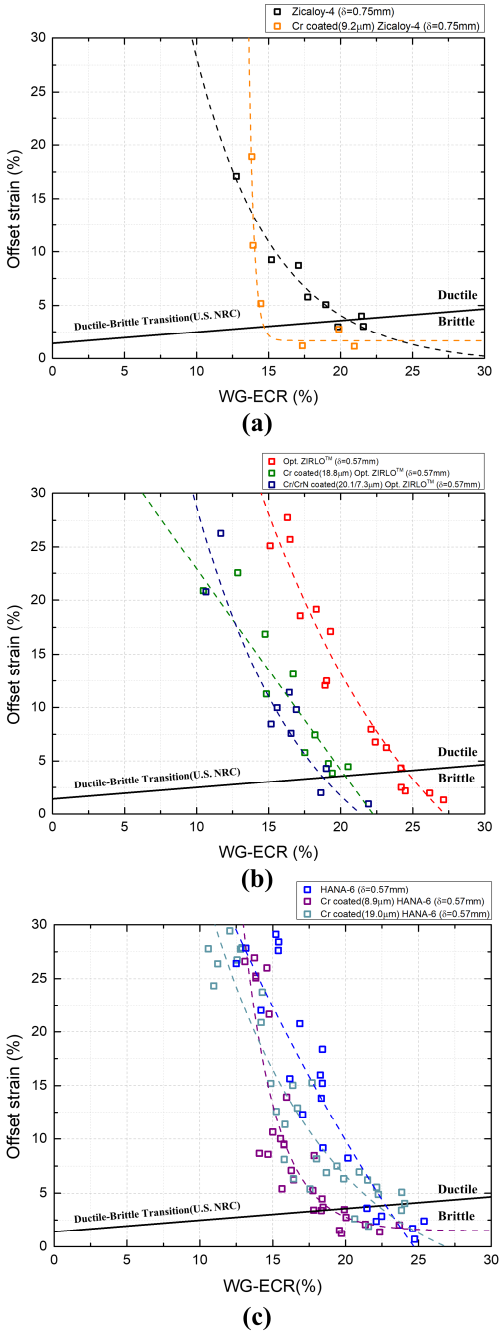

Fig. A. measured WG-ECR to offset strain curve with ductile to brittle criteria from U.S. NRC. (a) Cr coating on Zircaloy-4 base material (b) Cr and Cr/CrN coating on Opt. ZIRLO™ base material (c) Cr coating on HANA-6 base material

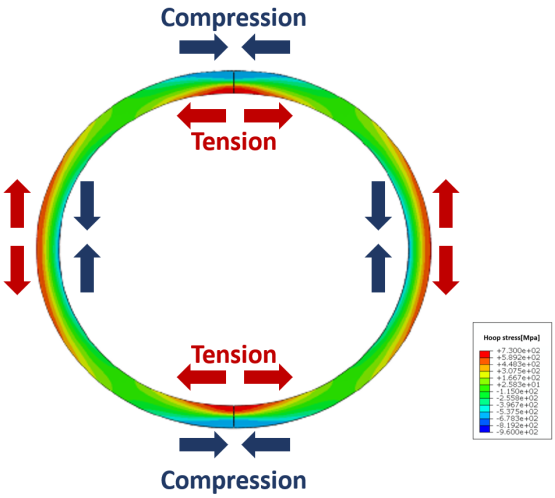

Fig. B. Stress distribution of cladding with a fairly cylindrical shape during RCT simulated by FEA.